BMC Cell Biology

Research article

Rapid degradation of dominant-negative Rab27 proteins *in vivo* precludes their use in transgenic mouse models

José S Ramalho[1], Ross Anders[1], Gesine B Jaissle[2], Mathias W Seeliger[2], Clare Huxley[1] and Miguel C Seabra*[1]

Address: [1]Cell and Molecular Biology, Division of Biomedical Sciences, Faculty of Medicine, Imperial College, Sir Alexander Fleming Building, Exhibition Road, London, SW7 2AZ, UK and [2]Department of Pathophysiology of Vision and Neuropthalmology, University Eye Hospital, Tübingen, Germany

E-mail: José S Ramalho - ramalho@imagem.ibili.uc.pt; Ross Anders - r.anders@ic.ac.uk; Gesine B Jaissle - see@uni-tuebingen.de; Mathias W Seeliger - see@uni-tuebingen.de; Clare Huxley - c.huxley@ic.ac.uk; Miguel C Seabra* - m.seabra@ic.ac.uk

*Corresponding author

Abstract

Background: Transgenic mice have proven to be a powerful system to study normal and pathological gene functions. Here we describe an attempt to generate a transgenic mouse model for choroideremia (CHM), a slow-onset X-linked retinal degeneration caused by mutations in the Rab Escort Protein-1 (REP1) gene. REP1 is part of the Rab geranylgeranylation machinery, a modification that is essential for Rab function in membrane traffic. The loss of REP1 in CHM patients may trigger retinal degeneration through its effects on Rab proteins. We have previously reported that Rab27a is the Rab most affected in CHM lymphoblasts and hypothesised that the selective dysfunction of Rab27a (and possibly a few other Rab GTPases) plays an essential role in the retinal degenerative process.

Results: To investigate this hypothesis, we generated several lines of dominant-negative, constitutively-active and wild-type Rab27a (and Rab27b) transgenic mice whose expression was driven either by the pigment cell-specific tyrosinase promoter or the ubiquitous β-actin promoter. High levels of mRNA and protein were observed in transgenic lines expressing wild-type or constitutively active Rab27a and Rab27b. However, only modest levels of transgenic protein were expressed. Pulse-chase experiments suggest that the dominant-negative proteins, but not the constitutively-active or wild type proteins, are rapidly degraded. Consistently, no significant phenotype was observed in our transgenic lines. Coat-colour was normal, indicating normal Rab27a activity. Retinal function as determined by fundoscopy, angiography, electroretinography and histology was also normal.

Conclusions: We suggest that the instability of the dominant-negative mutant Rab27 proteins *in vivo* precludes the use of this approach to generate mouse models of disease caused by Rab27 GTPases.

Background

Membrane traffic in eukaryotic cells is mediated by vesicular carriers, which bud from a donor compartment, are targeted to, and fuse with the appropriate acceptor membrane. The Rab family of Ras-like GTPases is known to play a crucial role controlling these mechanisms [1,2]. Among Rabs, the Rab27 subfamily consists of two isoforms, Rab27a (previously designated Ram) [3] and Rab27b (previously designated c25KG) [4].

In order to function in membrane traffic, Rabs require the covalent addition of one or two C20 geranylgeranyl groups [5,6]. Geranylgeranylation serves as a membrane-anchoring device in Rab proteins [5]. This reaction is complex and occurs in several steps. Newly synthesised Rab proteins first associate with Rab Escort Protein (REP) and form a stable 1:1 complex [7,8]. The complex then serves as a substrate for Rab geranylgeranyl transferase to catalyse geranylgeranylation via thioether bonds to carboxy-terminal cysteine residues in Rabs [9,10]. Alternatively, newly synthesised Rabs can associate with a pre-formed REP:Rab-geranylgeranyl-transferase complex [11]. After geranylgeranylation, the REP:Rab complex is competent for delivery of the newly prenylated protein to cellular membranes by a process that has not been characterised [12,13].

The human genome contains two related REP genes, *REP1* and *REP2* [14]. Loss-of-function mutations in *REP1* result in choroideremia, an X-linked slow-onset retinal degeneration that affects photoreceptors, retinal pigment epithelium and the choroid [8,15]. We have speculated that the disease is caused by selective defects in Rab geranylgeranylation in the affected retinal cells and have identified Rab27a as one Rab that appears selectively unprenylated in choroideremia lymphoblasts [16]. Thus, Rab27a, which is expressed at high levels in the retinal pigment epithelium and choroid, could play an important role in triggering the degenerative process in choroideremia [16,17].

The rationale for the present study was to generate transgenic mice expressing dominant-negative mutant Rab27 proteins in order to interfere with the function of the wild type alleles and disrupt the Rab27 regulatory function. We found that dominant-negative Rab27 proteins are unstable and quickly degraded *in vivo*, and are thus unable to generate a dominant-interfering effect.

Results
Construction of transgenic vectors
Previous studies indicated that selective point mutations in Ras-like proteins that interfere with the cycle of GTP binding and hydrolysis produce either dominant-negative or constitutively-active mutant proteins [18]. Equivalent

mutations were introduced into Rab27a cDNA with the predicted effects indicated in Table 1. In order to study whether Rab27a played a role in the retinal degenerative process observed in choroideremia, we wished to generate transgenic mouse lines expressing dominant-negative Rab27a.

We constructed two sets of transgenic lines. For one set we took advantage of the tyrosinase tissue-specific promoter to drive expression of the transgene in pigmented cells including retinal pigment epithelium and choroidal melanocytes, given that these cell types are probably the primary site of degeneration in choroideremia [15,19,20]. cDNAs for Rab27a wild-type, dominant-negative mutants (Rab27a^{T23N} and Rab27a^{N133I}) and constitutively-active mutant (Rab27a^{Q78L}) were cloned downstream of the tyrosinase promoter and upstream of the human growth hormone. Figure 1A provides a schematic diagram of the PTyr/Rab27a/hGH expression constructs. These constructs include a 2,200-bp fragment of the tyrosinase promoter, a 650-bp rat Rab27a coding sequence and 600-bp of sequence derived from the human growth factor gene, which provides a polyadenylation signal. To generate transgenic lines, a 3.4 kb *Xho*I – *Not*I fragment containing the expression cassette was injected into (C57BL/6JxCBA) embryos according to standard procedures [21]. For the second set, we used the chicken β-actin promoter to achieve ubiquitous and high level expression of the transgenes in the mice [22,23]. Figure 1B provides a schematic diagram of the PCAG/myc-Rab27/β-globin expression constructs, which include a 1,235-bp fragment of chicken β-actin promoter, a 365-bp CMV-IE enhancer, a 33-bp myc-tag fragment, a 650-bp rat Rab27a or human Rab27b coding sequence and 525-bp of the rabbit β-globin polyadenylation signal. To generate transgenic lines, a 3.4-kb *Spe*I – *Bam*HI fragment containing each expression cassette was injected into (C57BL/6JxCBA) embryos according to standard procedures [21].

Production of transgenic lines
Transgenic lines generated following injection of the PTyr/Rab27a/hGH or PCAG/myc-Rab27/β-globin constructs were named according to the nomenclature indicated in Table 2. Mice containing the Rab27a transgenes were identified by PCR using primers specific to the tyrosinase promoter or myc-epitope (5' primer) and Rab27a cDNA (3' primer) (data not shown). In addition, each line was subjected to Southern blotting. Figure 2 shows a typical Southern blot screening following KpnI digestion and hybridisation using the entire coding sequence of Rab27a as a probe. Note that KpnI cuts the transgene once between the myc-tag and the coding sequence of Rab27a. Thus, a single transgenic integration will generate one hybridising fragment in addition to the endogenous bands. A tandem array of transgenes will generate two bands, one
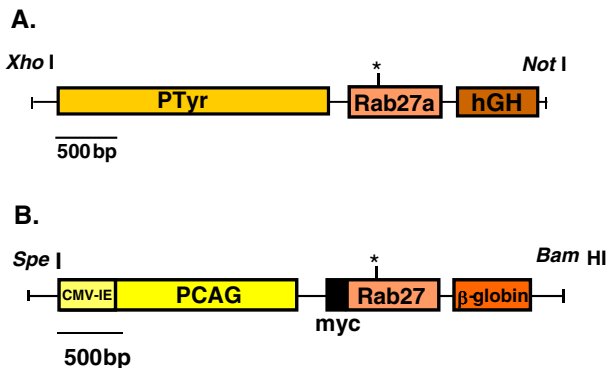
A.

B.

Figure 1
Organisation of transgenic constructs. Panel A depicts the PTyr/Rab27a/hGH constructs and Panel B depicts the pCAG/myc-Rab27/β-globin constructs generated as described under "Methods". Point mutations are indicated by an asterisk.

at 3.4 kb corresponding to the transgenic array and one of variable size corresponding to the Rab27a cDNA nearest the adjacent genomic DNA. As shown in Figure 2, DNA from mouse 21 showed a single extra band, suggesting a single integrated copy while DNA from mouse 25 exhibited one band at about 12 kb and one at 3.4 kb suggesting tandem integration. An accurate number of transgenic sequences per cell was not determined in part because the transgene expression was independent of transgene copy number, as previously reported [24,25]. For all the constructs injected, the germ line integration was approximately 20% and thus quite efficient. At least two founders that transmit each transgene were generated. All the founder animals (F0) obtained were successfully bred with C57BL/6J mice to establish transgenic lines. We also attempted to generate homozygous transgenic mice but this was only possible for a restricted number of lines.

Transgene mRNA expression
The expression of the transgenes was initially assessed using an RT-PCR assay on total RNA extracted from eye tissue (Fig. 3). We designed an assay where both transgenic and endogenous Rab27a mRNA could be amplified by selecting primers that would anneal equally well to the mouse and rat sequences. The RT-PCR products were then digested with EcoRI (cutting only the rat sequence) or SmaI (cutting only the mouse sequence) restriction enzymes to distinguish between endogenous and transgenic-derived products (Fig. 3A). This assay allowed us to distinguish between lines that do not express significant amounts of the transgene, such as A27aT25/1 from those that express high levels, such as A27aT25/2 (Fig. 3B). Al-

most all actin promoter-driven transgenic lines expressed high levels of transgenic mRNA as revealed by this assay. To quantify approximately the level of expression, the Rab27a or Rab27b product was compared to Hprt product (Fig. 3C and Table 3). All actin promoter-driven transgenic lines tested, except A27aT25/1, appeared to express the transgene at significant levels, approximately 3–12 times higher than the endogenous counterpart. Conversely, the expression levels in tyrosinase promoter-driven transgenes were much lower, typically not exceeding 3-fold over the endogenous levels (data not shown).

Transgenic protein expression by immunoblotting
The pCAG/myc-Rab27/β-globin expression constructs carry a myc tag fused to the Rab27 protein, which allowed the transgenic protein to be easily quantified. We prepared spleen lysates from transgenic mice and subjected them to immunoblotting analysis. Spleen was chosen because it contains relatively high amounts of endogenous Rab27a, which could be used as an internal control [16]. We used initially a specific monoclonal anti-Rab27a antibody, 4B12 as a probe and observed a 27-kDa band corresponding to the endogenous Rab27a protein in all lysates tested (Fig. 4A). In addition, a slower migrating band was also detected in samples prepared from some of the transgenic mice, corresponding to the myc-tagged transgenic protein as confirmed by immunodetection using the anti-myc antibody (Fig. 4B). To assess the range of tissues in which transgenic protein was expressed, twelve different organs (eye, spleen, liver, skin, lung, kidney, stomach, large intestine, small intestine, brain, testis and heart) were harvested and subjected to Western blotting analysis using anti-Rab27a or anti-myc specific probes. Examples where lines A27aQ24 (Rab27a^{Q78L}) and A27aT25/2 (Rab27a^{T23N}) were analysed are presented in Figure 4. The pCAG/myc-Rab27/β-globin constructs carrying the wild-type and constitutively-active mutant (Rab27a^{Q78L}) forms of Rab27a were found to express transgenic protein ubiquitously and at very high levels, usually more than ten times the endogenous levels (Fig. 4B and data not shown). In contrast the pCAG/myc-Rab27/β-globin constructs carrying dominant negative mutant Rab27a^{T23N}, Rab27a^{NI33I}, Rab27b^{T23N} and Rab27b^{NI33I} gave much lower levels of protein. The highest levels of dominant negative protein were observed in the line A27aT25/2 as shown in Fig. 4A. The amount of transgenic protein expressed in A27aT25/2 was relatively constant from tissue to tissue. In tissues where endogenous Rab27a expression was high, the levels of Rab27a^{T23N} transgenic protein were nearly equal to or lower than, but never higher, than endogenous protein (Fig. 4B). Lower levels of transgenic protein expression were observed for the other lines expressing dominant-negative mutant Rab27a and Rab27b (data not shown).
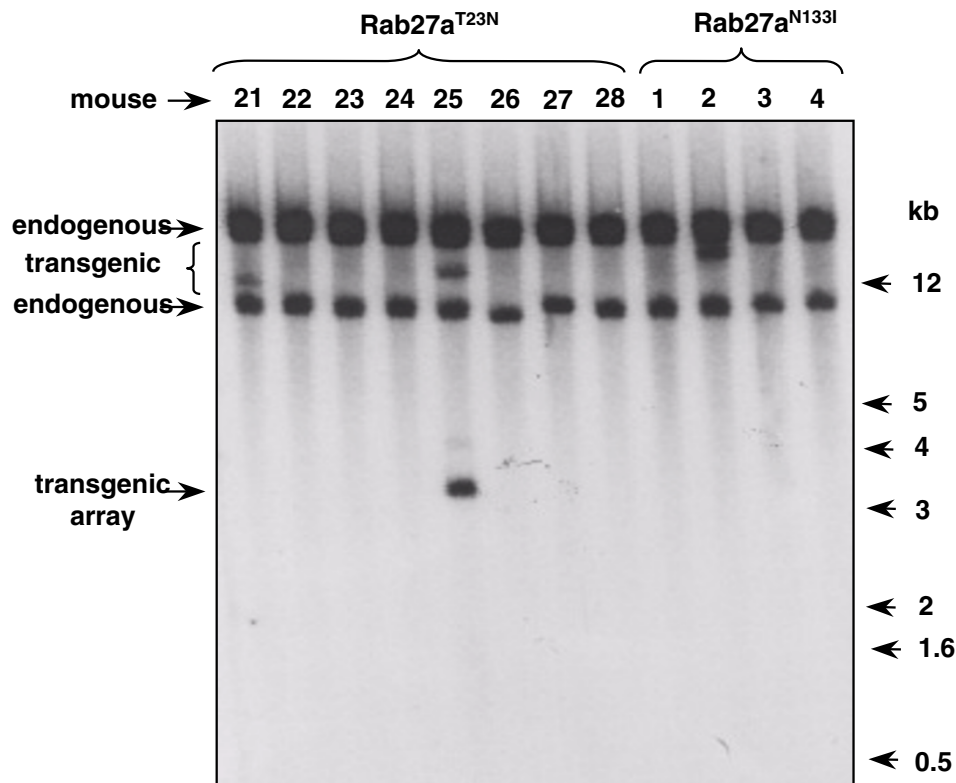
Figure 2
Screening of transgenic mice. Southern analysis was performed using mouse genomic DNA extracted from the tail of potential Rab27a[T23N] and Rab27a[N133I] transgenics. Each well contains genomic DNA extracted from an individual mouse tail biopsy and electrophoresed on an agarose gel as described under "Methods". The band around 3.4 kb suggests the presence of an array of transgenes.

The results for the tyrosinase promoter-driven transgenes were less clear as the transgenic protein did not contain an epitope tag and could not be distinguished from the endogenous protein. We have not been able to detect differences in the levels of Rab27a in any of the twelve tissues described above (data not shown).

Turn-over of Rab27a mutants
The discrepancy between mRNA levels and protein levels observed in the different transgenic lines suggested that some mutant proteins might be unstable and rapidly degraded. To explore this possibility, we performed a pulse-chase experiment to determine the approximate half-lives of the transgenic proteins. COS-7 cells were transfected with pCAG/myc-Rab27/β-globin constructs expressing either Rab27a[WT], Rab27a[Q78L], Rab27a[T23N] or Rab27a[N133I], then metabolically labelled with [35S]methionine/

cysteine for 1 h, followed by different time intervals of chase in the presence of non-radiolabelled medium. The cells were then harvested, lysed and subjected to anti-Rab27a immunoprecipitations. Under these conditions, we observed that both myc-tagged wild type Rab27a and Rab27a[Q78L] decayed with a half-life of approximately 24 h (Fig. 5A,5C,5E). In contrast, the dominant-negative mutant proteins exhibited much shorter half-lives. Our results indicate that the half-life of myc-Rab27a[T23N] is approximately 2.5 h while that of myc-Rab27a[N133I] is approximately 6 h (Fig. 5B,5D,5E). These results suggest that dominant-negative Rab27a mutants are unstable and degrade rapidly in comparison with wild type Rab27a.

Phenotypic characterisation: coat colour
While this work was in progress, Jenkins and co-workers reported that a Rab27a loss-of-function mutation leads to
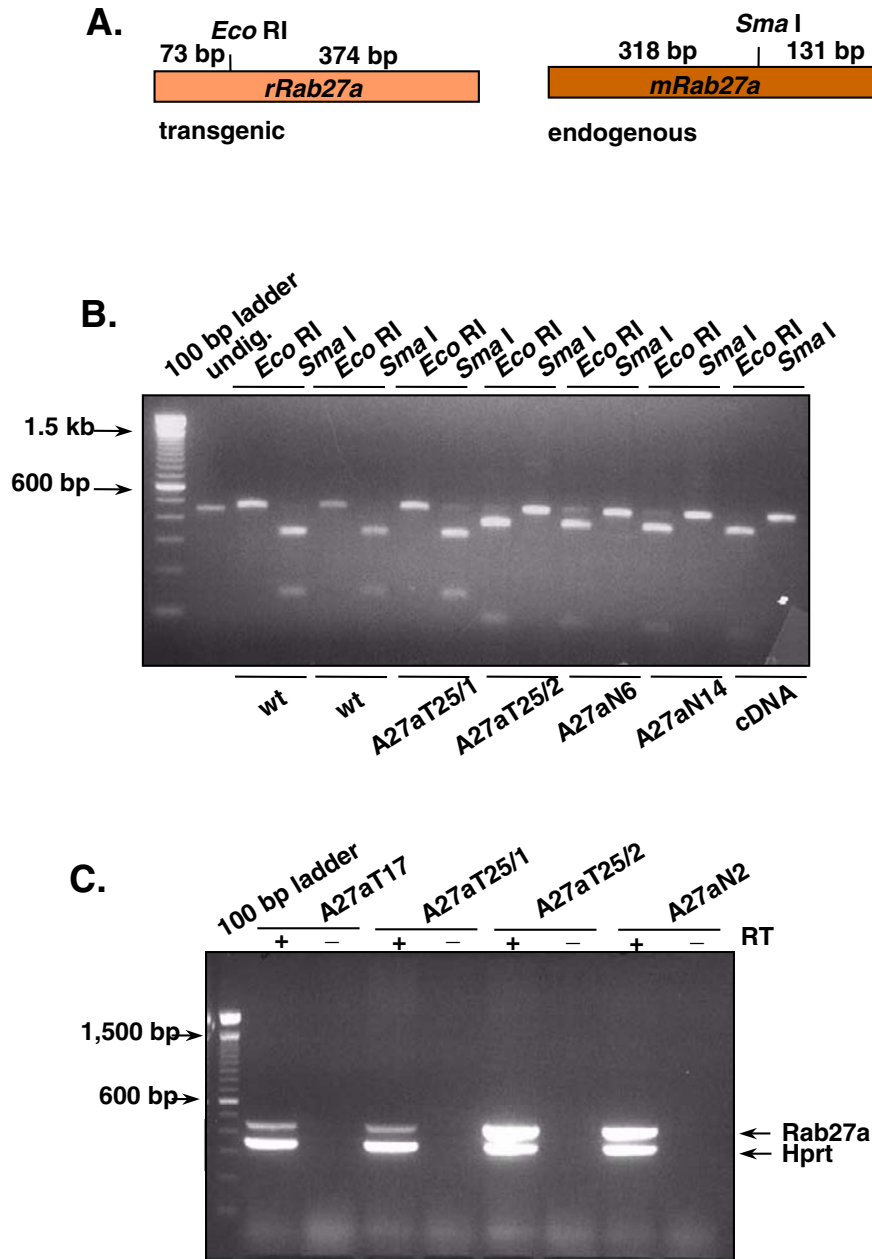
A.

B.

C.

Figure 3
Detection of Rab27a mRNA. (Panel A) Schematic depiction of transgenic (rat) versus endogenous (mouse) Rab27a coding sequence. *Eco*RI or *Sma*I restriction sites as well as resulting fragment sizes are indicated. (Panel B) Comparison of transgenic versus endogenous Rab27a expression in the eye by RT-PCR and restriction digestion of PCR products. Rab27a mRNA from wild-type and independent mutant transgenic lines (Rab27a^{T23N} and Rab27a^{N133I}) amplified by RT-PCR was digested with *Eco*RI or *Sma*I and electrophoresed as described under "Methods". Rat Rab27a cDNA was used as a control. (Panel C) Determination of Rab27a expression (transgenic and endogenous) in eyes by RT-PCR (+). The oligonucleotides and conditions were as described under "Methods". The PCR products were analysed on an agarose gel stained with ethidium bromide. Reactions performed without reverse transcriptase are indicated (-). The arrows on the left-hand side indicate the positions of DNA marker sizes. Hprt expression was used as an internal control.

Table 1: Mutations affecting the GTP/GDP cycle of Rab27a

Rab27a mutation	expected biochemical properties	expected effect
T23N	preferential binding of GDP	dominant-negative
Q78L	reduced GTPase activity	constitutively-active
N133I	low affinity for GDP/GTP	dominant-negative

Table 2: Nomenclature for transgenic lines

promoter	mutant Rab27	transgenic line identification*
tyrosinase	Rab27a^{T23N}	T27aT*
	Rab27a^{Q78L}	T27aQ
	Rab27a^{N133I}	T27aN
β-actin	Rab27a^{T23N}	A27aT
	Rab27a^{Q78L}	A27aQ
	Rab27a^{N133I}	A27aN
	Rab27a wt	A27awt
	Rab27b^{T23N}	A27bT
	Rab27b^{N133I}	A27bN
	Rab27b wt	A27bwt

* T – T23N; Q – Q78L and N – N133I; when multiple lines were obtained for the same construct these are identified numerically.

the phenotype observed in the *ashen* mouse [26]. The *ashen* mouse is a model for Griscelli Syndrome (GS), which is caused by Rab27a mutations [26,27]. The phenotype of GS is characterised by partial albinism (coat colour dilution in the mouse) and loss of cytotoxic T-lymphocyte (CTL) killing activity resulting in immunodeficiency. We therefore predicted that our transgenic mice expressing dominant-negative Rab27a mutants would show coat colour dilution if a dominant-negative effect had resulted *in vivo*. Figures 6A and 6B show representative photographs of dominant-negative mutant transgenic mice, demonstrating no apparent lightening of coat colour similar to that seen in *ashen* mice. Coat colour dilution in *ashen* mice is probably due to defects in distribution of melanosomes in skin melanocytes. However, microscopic examination of hair shafts from mutant Rab27a transgenic animals revealed no clusters of aggregated melanin in follicular melanocytes similar to those observed in *ashen* skin (data not shown). In addition, the Rab27a^{Q78L} and wild-type transgenic mice expressing very high levels of transgenic protein did not present any obvious skin alterations (data not shown).

To test the functionality of the transgenic Rab27a proteins *in vivo*, we produced mice where the transgenic protein was the only source of Rab27a. This was accomplished by crossing the transgenic lines twice with *ashen* homozygous mice to obtain homozygous *ashen* mice carrying the transgenes. The offspring were genotyped [28] and examined for coat colour. As expected, the wild-type Rab27a transgene was able to rescue the *ashen* mice coat colour nearly completely (Fig. 6C) while the dominant-negative Rab27a^{T23N} transgene did not (Fig. 6D). Mice that were homozygous for the *ashen* mutation and carried the constitutively-active mutant Rab27a^{Q78L} transgene (*ash/ash*, -/tg^{Rab27aQ78L}) partially rescued the coat colour defect (Fig. 6D). This effect was strengthened by transgene homozygosity. Transgenic *ash/ash*, tg^{Rab27aQ78L}/tg^{Rab27aQ78L} mice were almost entirely rescued to wild type coat colour (data not shown).

Phenotypic characterisation: vision
Despite the lack of a coat colour phenotype, we decided to study retinal function in the transgenic mice. These studies included fundoscopy, angiography, electroretinography and histology and were performed at different ages, from 1 month to over 1 year old.
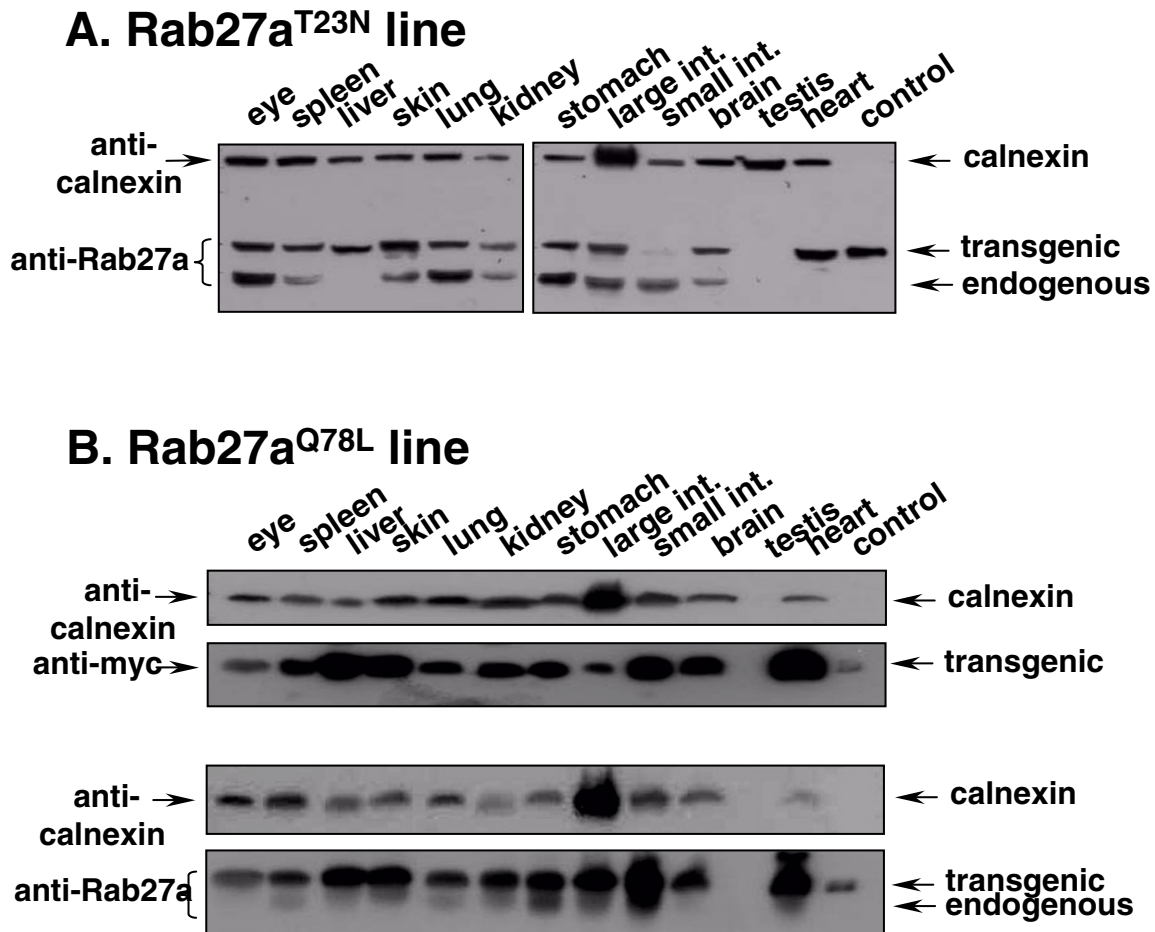
A. Rab27a^{T23N} line

B. Rab27a^{Q78L} line

Figure 4
Expression of transgenic Rab27a proteins in mouse tissues. Protein extracts obtained from eyes, spleen, liver, skin, lung, kidney, stomach, large intestine, small intestine, brain, testis and heart (50 μg each) were subjected to SDS-PAGE and probed with monoclonal anti-myc-tag antibody (9E10) and/or a specific anti-Rab27a monoclonal antibody (4B12). Calnexin was used as a loading control and detected using a specific polyclonal antibody. A protein extract of HeLa cells transfected with myc-Rab27a^{T23N} was used as a positive control. (Panel A) Tissues from the A27aT25/2 line carrying Rab27a^{T23N}. (Panel B) Tissues from the A27aQ24 line carrying Rab27a^{Q78L}.

Fundoscopy is a method that allows detection of gross abnormalities such as retinal or subretinal deposits, defects in the RPE, new vascularisation and detachments of the retina. The system allows rapid, inexpensive and serial examination of the retina and also obtaining very high quality images of the posterior segment of the mouse eye. Figure 7 shows representative photographs of wild type (C57BL/6J) and transgenic (Rab27a^{T23N}) mice at 6 months of age. The examination of the fundus of transgenic mice revealed regular pigmentation at the level of the RPE. The optic nerve and retinal blood vessels in fundus seemed to be normal. Fundi of mice from all transgenic lines have been examined up to one year old and no

significant alterations have been detected, with one exception. The T27aT15 line exhibited extensive pathological alterations in both the anterior and posterior segments of the eye, which were probably caused by the disruption of one or more genes at the site of transgene insertion (J.S. Ramalho and M.C. Seabra, manuscript in preparation).

The retinal vasculature was examined by fluorescein angiography, i.e., fundus photography combined with intravenous fluorescein injection [29]. Neovascularisation that is often present in retinal degeneration is easily identified. It is also possible to detect defects in the RPE, since the melanin in the RPE can attenuate the fluorescence from the
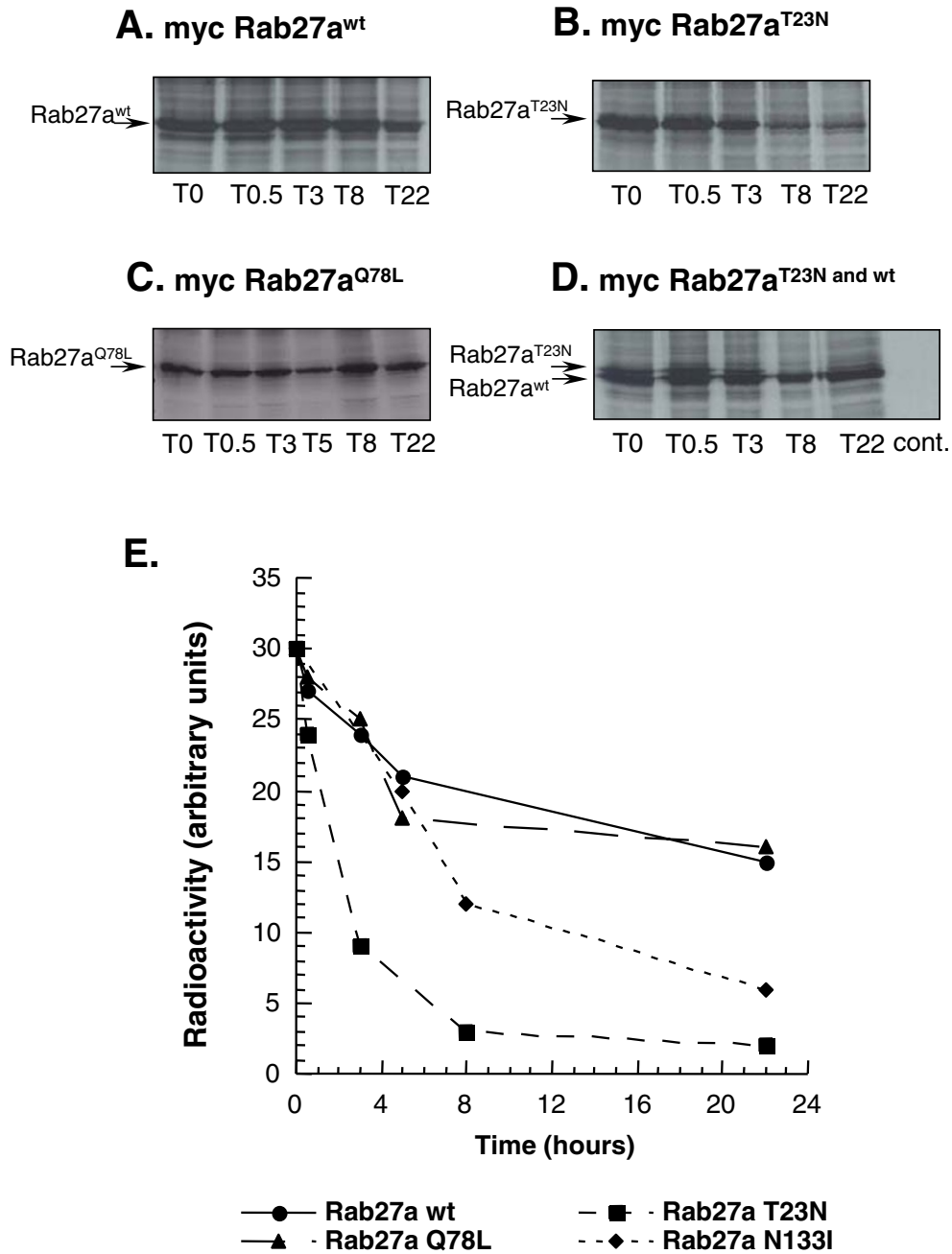
Figure 5
Half-lives of wild-type, Rab27a^{T23N}, Rab27a^{Q78L} and Rab27a^{N133I} mutant proteins. COS-7 cells transfected with either pCAGGS myc-Rab27a^{WT} (A), pCAGGS myc-Rab27a^{T23N} (B), pCAGGS myc-Rab27a^{Q78L} (C), or co-transfected with pCAGGS myc-Rab27a^{WT} and pCAGGS myc-Rab27a^{T23N} (D) were labelled with [^{35}S]methionine/cysteine for 2 h and subsequently chased in Dulbecco's modified Eagle's medium for the indicated times. Rab27a protein was immunoprecipitated from cell extracts, collected with protein G-Sepharose beads, separated on a 12% SDS-polyacrylamide gel and autoradiographed as described under "Methods". (Panel E) Quantification of radiolabelled samples obtained above.

Table 3: Transgenic protein and mRNA expression.

Rab27 mutant	line	mRNA expression*	transgenic protein expression
Rab27a^{T23N}	T27aT2	0.20 ± 0.02	not detectable
	T27aT15	0.29 ± 0.03	not detectable
	T27aT17	0.31 ± 0.01	not detectable
	T27aT20	0.29 ± 0.01	not detectable
	A27aT6	2.6 ± 0.2	++
	A27aT6/18	not determined	++
	A27aT13	1.8 ± 0.1	
	A27aT25/1	0.21 ± 0.03	
	A27aT25/2	1.7 ± 0.1	+++
Rab27a^{Q78L}	T27Q102	0.32 ± 0.06	
	A27aQ13	not determined	§
	A27aQ24	not determined	§
Rab27a^{N133I}	T27aN14/5	0.61 ± 0.02	not detectable
	T27aN48	0.26 ± 0.02	not detectable
	A27aN2	0.95 ± 0.04	+
	A27aN6	1.27 ± 0.08	+
	A27aN14	2.2 ± 0.4	not detectable
Rab27a wt	A27aTwt2	not determined	+++
Rab27b^{T23N}	A27bT40	1.21 ± 0.03	+
	A27bT59	0.6 ± 0.1	not detectable
Rab27b^{N133I}	A27bN9	1.64 ± 0.06	++

+++ represents transgenic Rab27 protein level similar to endogenous, ++ or + represent transgenic Rab27 protein level below endogenous, §very high levels of transgenic protein compared to endogenous; * mRNA Rab27 values are expressed as (endogenous + transgenic Rab27a or Rab27b) / Hprt. Endogenous Rab27a/Hprt = 0.22 ± 0.01. Endogenous Rab27b/Hprt = 0.12 ± 0.01.

choroidal circulation. Figure 8 depicts representative examples of fluorescein angiography from Rab27a^{T23N} transgenic mice (A27aT25/2 line) and wild-type litter mates. The retinal vessels are clearly visualised 30 s after injection. We observed no narrowing vessels, no abnormal leakage of fluorescein dye from the retinal capillaries and no hyperfluorescence of the retinal pigment epithelium.

Another important complementary method of eye examination is Ganzfeld electroretinography (ERG). In a Ganzfeld setup, the stimulus (usually a Xenon tube flash of less than 1 ms duration) passes through a diffusor that yields a relatively homogeneous distribution of light intensity on the inside of a bowl. The term 'Ganzfeld' meaning 'full field' denotes that the stimulus reaches practically all parts of the retina and its intensity is approximately equal across that area. For most applications, the ERG, which is an electric sum potential generated by retinal cells following exposure to light, is non-invasively measured at the corneal surface. Typically, the evoked response consists of an initial negative deflection (a-wave), followed by a large, positive component (b-wave). Superimposed on the ascending portion of the b-wave are the oscillatory potentials (OPs), a set of wavelets oscillating with approximately 4–5 times the frequency of the a- and b-wave. Finally, a prolonged positive component (c-wave) follows, which takes several seconds to develop.

Due to characteristic contributions of photoreceptors, bipolar cells, and amacrine cells, the ERG is a valuable indicator of retinal function beyond the ganglion cell level. To
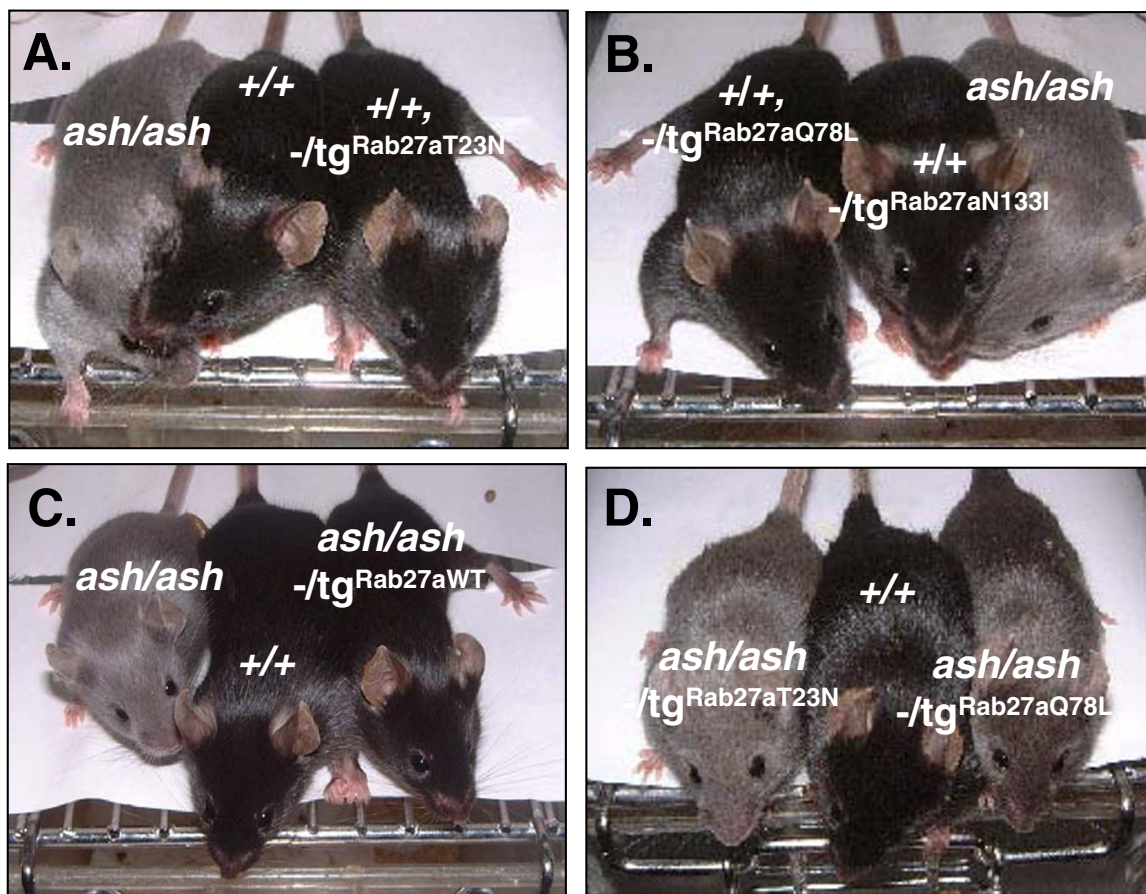
Figure 6
Photographs of representative transgenic and mutant mice. +/+, wild type C57BL/6J mouse; *ash/ash*, homozygous *Rab27a*ashen mutant mouse; -/tg, heterozygous transgenic of the indicated line.

assess whether potential functional changes in the transgenic lines could be picked up with this method, the lines that presented higher levels of transgenic protein were subjected to ERG at six months of age. Representative lines from each transgenic construct were analysed at six months and found to be indistinguishable from wild type in all but one case. In A27aT25/2 mice (Rab27a^{T23N}), the b-wave amplitudes were all in the low-normal range (Fig. 9) but these differences were not statistically significant. Interestingly, this transgenic line showed the highest level of dominant-negative transgenic protein and thus the low-normal ERG may have resulted from a dominant-negative effect of mutant Rab27a. However, as only one of the lines studied showed this result, the disruption of a gene with important function in the retina upon transgenesis in the A27aT25/2 appears to be the most likely explanation.

Finally, we performed histological analysis. Retinal cross-sections subjected to conventional histochemical staining taken from 10 month old Rab27a^{T23N} (A27aT25/2 line) and littermate control are shown in Figure 10. Again, we observed no significant differences between the control and the Rab27 transgenic animals. Note the normal thickness of the outer nuclear layer, reflecting normal numbers of photoreceptors in the retina.

Discussion

At the outset, we wished to investigate the possible role of Rab27 proteins in human disease, in particular CHM. We decided to generate transgenic mice expressing dominant-negative forms of Rab27 for several reasons. Firstly, the strategy of generating Rab proteins defective in either GTP hydrolysis (constitutively-active) or GDP/GTP exchange (dominant-negative) to selectively alter the function of individual Rab proteins in cultured cells has been extensively used previously (for example [30,31]). In some cases,
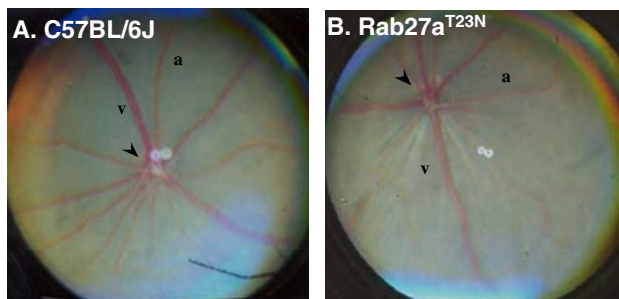
Figure 7
Photographs of the fundus of the Rab27a^{T23N} transgenic mouse. Wild-type (C57BL/6J control littermate) (**A**) and Rab27a^{T23N} transgenic mouse (A27aT25/2 line) (**B**) were photographed at 6 months of age as described under "Methods". The venules (v) are twice the diameter of the arterioles (a). The optical nerve head is indicated by an arrow. Note that the two white dots are result of light reflection on the lens between the camera and the mouse's eye.

these mutants have had profound effects on membrane trafficking such as with Rab5 [31], but in others such as Rab11a the effects were more subtle [32]. Secondly, a transgenic approach to express the equivalent Rab5 dominant-negative mutant, Rab5^{N133I} in immune cells reportedly resulted in the desired phenotype [33]. Thirdly, this approach was the best model for studying the partial dysfunction of Rab27a observed previously since dominant-negative proteins would unlikely inactivate 100% of wild type activity [15,16]. In addition, the dominant-negative approach could also result in inactivation of Rab27b activity, if not other related proteins. In contrast, a gene knock-out approach would result in complete absence of Rab27a while retaining full activity of the related protein Rab27b. Our recent finding that Rab27b shows functional redundancy with Rab27a further suggests that Rab27a-related Rabs may be involved in CHM [28]. Fourthly, we observed that these same Rab27a mutations were effective in cell culture models [34].

While this work was in progress, there was a considerable advance in understanding the function of Rab27a and its role in disease. Loss-of-function mutations in Rab27a were observed in patients with Griscelli syndrome (online Mendelian Inheritance in Man (OMIM) # 214450, [http://www.ncbi.nlm.nih.gov/Omim/]) and in the corresponding mouse model, *ashen* [26,27]. GS is a rare, lethal autosomal recessive disorder, characterised by pigment

dilution of the hair (and to a lesser extent of skin) together with early-onset immune deficiency with episodes of hemophagocytic (uncontrolled T lymphocyte and macrophage activation) syndrome [35,36]. The partial albinism in GS patients is due to clumping of melanin pigment in the hair shaft and accumulation of melanosomes around the nucleus within melanocytes [34–38]. The immune deficiency is due to loss of CTL killing activity [27,39,40]. If the Rab27a mutant proteins Rab27a^{T23N} and Rab27a^{N133I} acted as strong dominant-negative mutants, as they do in cell culture [34,38], the transgenic lines generated should exhibit a phenotype resembling *ashen* mice, possibly with additional phenotypes due to inactivation of Rab27b as well. Unfortunately, no phenotype could be detected in the transgenic lines. Coat colour was not affected (Fig. 5) and CTL activity could not be studied given that the β-actin promoter used in this study does not express in these cells [28]. We also performed detailed analysis of the retina in the transgenic lines, including fundoscopy, angiography, histology and ERG, and could not detect any significant pathological changes.

The lack of phenoytpe in the transgenic mice expressing dominant-negative mutant Rab27a and Rab27b could have been due to non-functional mutant proteins. However, this explanation seems unlikely as the same type of mutants are functional in cultured melanocytes [34,38]. It has been proposed that one mechanism for dominant-negative action by these mutations in Ras-like proteins is by competition for GDP/GTP exchange factors, required for activation of the endogenous proteins [18]. Thus, the absence of phenotype in these mice is probably due to inadequate levels of protein expression to elicit a dominant-negative effect. Indeed, out of more than twenty transgenic lines generated so far expressing dominant-negative mutant forms of Rab27a or Rab27b, only one (A27aT25/2) had transgenic protein levels close to the endogenous counterpart (Fig. 4B).

The low levels of dominant-negative transgenic protein are not due to poor expression of the transgenes as very high levels of mRNA was observed in many of the lines. In addition the wild-type and constitutively active proteins were present at high levels from similar constructs. The low levels of protein are probably due to more rapid turnover of the dominant-negative mutant proteins and we observed that the Rab27a^{T23N} and Rab27a^{NI33I} proteins have half-lives 4–8 times shorter than the wild type protein in tissue culture (Fig. 5). This fast turnover of the dominant-negative protein compared to the constitutively-active and wild-type proteins probably results from a combination of factors. The transgenic protein could be poorly prenylated, a possibility supported by the finding that only a small percentage of transgenic protein was membrane-associated (data not shown). Also, the muta-
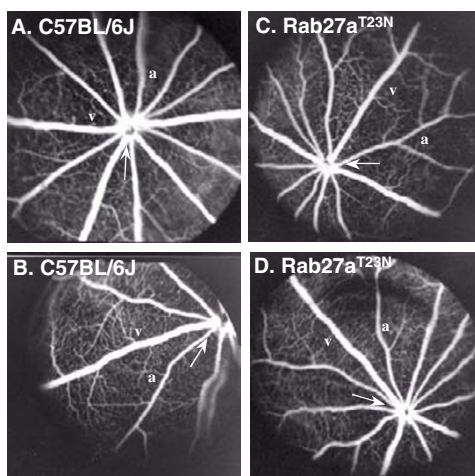
Figure 8
Fluorescein fundus angiograms of Rab27a^{T23N} transgenic mouse retina. Angiograms of six monthsold wild-type (C57BL/6J littermate control) (A and B) or Rab27a^{T23N} transgenic mouse (A27aT25/2 line) (C and D) taken one minute after dye injection were obtained as described under "Methods". The venules (v) are twice the diameter of the arterioles (a). The arrow denotes the optical nerve.

tion could reduce the stability of the tertiary structure of the mutant protein resulting in an increased rate of unfolding. Although the rate of turnover of Rab27b proteins was not determined, the low levels of dominant negative mutant protein in transgenic lines expressing high levels of mRNA suggests that Rab27b^{T23N} and Rab27b^{NI33I} also have high rates of turn-over. These observations *in vivo* contrast with the effects observed in cultured cells, where transient transfection leads to acute expression of very high levels of mutant proteins.

Our initial hypothesis that Rab27a plays a role in the retinal degenerative process of CHM remains untested given the lack of success of this approach. As we proposed originally, it is unlikely that Rab27a is the only dysfunctional Rab protein in this disorder and our inability to test retinal tissue from patients has hampered the identification of other Rabs that might be involved [16]. Nevertheless, the availability of Rab27a knock-out mice (*ashen*) may allow us to determine whether Rab27a plays an important role in retinal physiology and further elucidate the pathogenesis of CHM.

Conclusions
The results presented here suggest that the use of dominant-negative proteins in *in vivo* models should be carefully considered. We report the generation of several transgenic lines expressing dominant-negative mutants of Rab27a and Rab27b where no phenotype could be elicit-

ed. The lack of a phenotype is likely due to the very modest levels of protein expression, probably caused by rapid degradation, despite very high levels of mRNA resulting from transcription driven by a strong promoter in the transgene.

Methods
Animals
All animals described here were maintained on 12-h light/12-h dark conditions at Imperial College, CBS Unit, London, UK, under Home Office Project Licence 70/5071.

Construction of mutant Rab27a transgenic vectors
Two general transgenic constructs were constructed, the first contained the pigment cell-specific tyrosinase promoter, Rab27a cDNA and the human growth hormone poly A signal and the second contained the strong ubiquitous chicken β-actin promoter and CMV-IE enhancer (PCAG), followed by an amino-terminal myc-epitope-tagged version of Rab27a or Rab27b, followed by rabbit β-globin poly(A) signal (Fig. 1). The construction of the first transgenic vector was initiated by subcloning a *Bam*HI – *Not*I fragment containing the human growth factor (hGH) termination sequence [41,42] (a generous gift from David Russell, University of Texas Southwestern Medical Center, Dallas, USA) into pBS containing a 2.2 kb insert corresponding to mouse tyrosinase promoter (a generous gift from Paul Overbeek, Baylor College of Medicine, Houston, USA) [19,20]. For the second transgenic construct, the promoter and poly A regions were from pCAGGS [22,23]. The point mutations, Rab27a^{T23N}, Rab27a^{N133I}, Rab27a^{Q78L}, Rab27b^{T23N} and Rab27b^{N133I} were generated by PCR mutagenesis using the rat Rab27a or the human Rab27b cDNA as a template. The myc-epitope was inserted in frame into the Rab27 cDNA by subcloning the Rab27 cDNA into pCMV7-MYC [43] or pBS-MYC. pBS-MYC was generated by cloning the *Cla*I/*Sal*I-fragment from pCMV7-MYC containing the myc-epitope into pBluescript SK. The fragments containing the myc-Rab27 cDNA were excised from pCMV7-MYC or pBS-MYC with *Xba*I and *Bam*HI or *Xho*I and *Bam*HI, respectively. After gel purification using QIAquick Gel Extraction Kit (Qiagen), the recessed 3' termini were filled with 0.5 U of Klenow fragment of *Escherichia coli* DNA polymerase I according to the manufacturer's instructions. The product was then subcloned into the blunted *Xho*I site of pCAGGS after Klenow fragment treatment (Fig. 1A).

Generation of the transgenic mice
A 3.4 kb *Xho*I – *Not*I fragment containing the Ptyr/Rab27a/hGH or a 3.4 kb *Spe*I – *Bam*HI fragment containing PCAG/myc-Rab27/β-globin were gel purified using QIAquick Gel Extraction Kit (Qiagen) as described by the manufacturer and eluted with 10 mM Tris-HCl (pH 8.5). DNA was then dissolved in sterile 0.1 mM EDTA, 10 mM
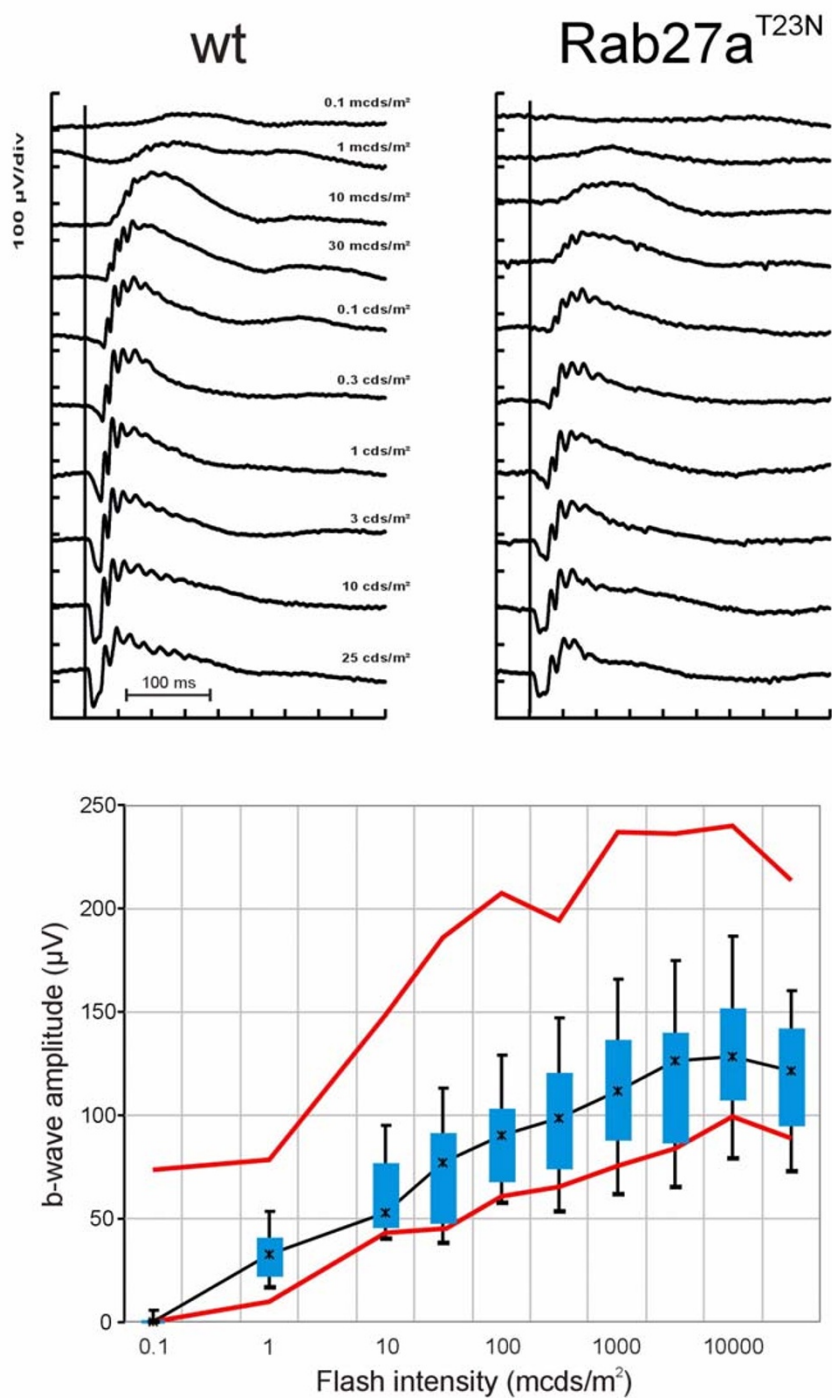
Figure 9
Electrophysiological characteristics of the A27aT25/2 transgenic mouse line. (Panel A) Dark-adapted (scotopic) intensity series of a six month-old wild-type control (left column) and a A27aT25/2 transgenic mouse (right column). Calibration marks: Vertical 100 µV/div.; horizontal 40 ms/div. Stimulus intensities increased from top to bottom from 10^{-4} to 25 cd*s/m². (Panel B) Amplitude vs. intensity plot for the A27aT25/2 transgenic line in comparison to wild type mice. The crosses indicate the median, the boxes the 25%- to 75%-quantiles, and the whiskers the 5%- to 95%-quantiles. The upper (95% quantile) and lower (5% quantile) red line indicate the normal range based on wild type data.
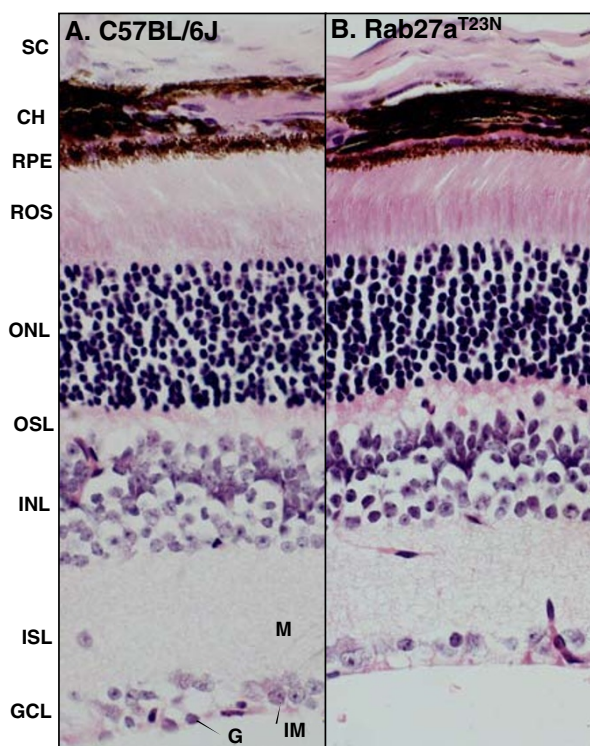
Figure 10
Histochemical staining of Rab27a^{T23N} transgenic mouse retina. Transverse paraffin sections (3 μm) from 10 month-old C57BL/6J (**A**) or Rab27a^{T23N} transgenic mouse (line A27aT25/2) (**B**) are shown. Magnification is approximately ×250. The abbreviations used are: sclera (SC), choroid (CH), retinal pigment epithelium (RPE), photoreceptor segments of rods and cones (ROS), nuclei of rods and cones (ONL), outer synaptic layer (OSL), neuron nuclear layer (INL), inner synaptic layer (ISL), ganglion cell layer (GCL), slender glial (Muller) cell processes (M), ganglion cells (G) and inner limiting membrane (IM).

Tris-HCl (pH 8.0) at about 2 ng/μl and microinjected into the pronuclei of one-cell stage embryos from a C57BL/6JxCBA background collected from super-ovulated female mice [21]. Microinjected eggs were transferred at two-cell stage into the oviducts of pseudopregnant recipient females. Newborn mice were routinely screened for incorporation of the transgene by PCR and/or Southern blotting.

Screening and generation of transgenic lines
Mice were genotyped by PCR amplification and by Southern blot analysis using genomic DNA obtained from mouse-tail biopsy samples. The transgene was detected with sense oligonucleotide JR119 (5'-ATGGAACAAAAACTCATCTCAGAAGAGG) corresponding to the myc-tag sequence of the transgene or JR13 (5'-ACATGTGATAGTCACTCCAGGGGTTGCT) corresponding to tyrosinase promoter, and antisense oligonucleotide JR14 (5'-AGTTGAACTTCCCATCAGTGTACTGGTA) corresponding to the Rab27a coding sequence. Tail biopsies (~ 0.5 cm) were digested with 40 μg/ml of proteinase K in 500 μl of extraction buffer containing 100 mM Tris-HCl (pH 8.0), 200 mM NaCl, 5 mM EDTA and 0.2% SDS overnight at 55°C followed by phenol/chloroform extraction. After precipitation with isopropanol, DNA was washed with 80% ethanol and resuspended in 50 μl of 10 mM Tris-HCl (pH 8.5). For Southern blotting, approximately 20 μg of tail genomic DNA was digested with *Kpn*I overnight at 37°C. DNA was separated on a 0.8% TAE agarose gel overnight at 120 mA and blotted onto Hybond-N+ (Amersham) membrane. Membranes were prehybridised and hybridised with Rab27a or Rab27b probe, corresponding to the entire Rab27 coding sequence, radiolabelled with 20 μCi of [α-^{32}P]dCTP by Random Oligopriming (Amersham). In order to generate stable transgenic lines, animals shown to be transgenic were subsequently mated to wild-type C57BL/6J mice; transgene-positive offspring (black colour mice) from these crosses were likewise bred. Transgenic lines were maintained as heterozygotes. Transgenic mice (Rab27^{T23N}, Rab27a^{Q78L} and Rab27a^{WT}) were crossed with *ashen* (*ash/ash*) on a C57BL/6J background obtained by repeated backcrossing of *ash/+* mice (over five generations) with wild-type C57BL/6J mice [28]. The resulting heterozygous *ashen* (+/*ash*) mice carrying the transgene were intercrossed to generate mice that carried the transgene on the *ash/ash* background. These mice were visually evaluated for the rescue of the coat colour. The *ashen* mutation was screened for by PCR using the primers ASH1 (5'-ACCTGACAAATGAGCAAAGTTTCCTCAATG) and ASH2 (5'-GGAGCAGGGCAGGGCTGGGGAAACCACTCG) followed by restriction enzyme analysis with *Taq*I and *Rsa*I according to the procedure described previously [28].

RT-PCR analysis
RT-PCR was carried out on total RNA obtained from eyes and isolated using RNeasy (Qiagen). After total RNA isolation, samples were treated with 1 U RNase-free DNase for 45 min at 37°C to remove any transgenic DNA contamination. The DNase was inactivated by heating for 15 min at 70°C. cDNA synthesis and DNA amplification were carried out using 5 μg of total RNA. Labelling of the PCR amplification product was carried out by addition of 0.025 μCi of [α-^{33}P]dATP. DNA was amplified using only 23 cycles (exponential phase). PCR amplification of Rab27a cDNA was performed with oligonucleotides JR62 (5'-GCATTGATTTCAGGGAAAAGAGAG) and JR63 (5'-

TTCTCCACACACCGCTCCATCCGC). To ensure that both transgenic and endogenous mRNA were amplified equally, these oligonucleotides were designed to be homologous to both endogenous (mouse) and transgenic (rat) Rab27 cDNA. After amplification, the PCR products were digested with *Eco* RI or *Sma* I to distinguish the mouse endogenous from rat transgenic cDNA. In most cases, the transgene expression was much higher than the endogenous expression making quantification impossible. Therefore, the transgene expression level was determined in each line by quantitating the Rab27 (endogenous plus mutant mRNA) relative to Hprt cDNA using all four primers, 0.025 μCi of $[\alpha$-$^{33}P]$ dATP and 23 cycles in PCR reaction. The oligonucleotides used for Hprt amplification were Hprt1 (5'-CCTGCTGGATTACATTAAAGCACTG) and Hprt2 (5'-GTCAAGGGCATATCCAACAACAAAC). Possible contamination of mRNA with transgenic DNA was excluded by control reactions without reverse transcriptase. The radiolabelled PCR products were separated on 2.5% agarose gels, stained with ethidium bromide, transferred onto 3 MM Whatman paper and quantified using a Cyclotron Storage Phosphor Screen (Packard).

Immunoblot analysis
Immunoblotting was performed according to procedures described elsewhere [16] with some modifications using total, cytosol or membrane protein fractions obtained from several C57BL/6J wild-type or transgenic tissues. All the transgenic and non-transgenic mice used for immunoblotting studies were thoroughly perfused with phosphate-buffered saline (PBS) (pH 7.4) prior to dissection of the tissue samples that included eye (the lens was always removed from the ocular globe), spleen, liver, lung, kidney, skin, stomach, large intestine, small intestine, brain, testis and heart. Tissue samples were washed with PBS, and thoroughly homogenised using a Polytron homogeniser in 3–5 volumes of homogenisation buffer containing 50 mM Tris-HCl (pH 7.5), 100 mM NaCl, 1 mM phenyl-methylsulfonyl fluoride, 10 μg/ml leupeptin, 10 μg/ml aprotinin, 10 μg/ml pepstatin and 1 mM DTT. Homogenisation was followed by sonication for 5–10 seconds. To sediment unbroken cells and cell nuclei, the homogenates were centrifuged at 5,000 g for 30 min at 4°C. The postnuclear supernatant was then centrifuged at 100,000 g for 1 h at 4°C, resulting in the separation of cytosolic (supernatant) and membrane (pellet) protein fractions. The membrane fractions were resuspended into the same volume of homogenisation buffer containing 1% Triton X-100. The protein concentration was determined only in the total fraction by BCA method (Pierce) according to the manufacturer's instructions. For immunoblot analysis, samples containing 50 μg of protein were separated into soluble or membrane fractions and identical volumes were subjected to SDS gel electrophoresis. After being resuspended into loading buffer, protein samples were loaded onto 12.5% SDS-polyacrylamide electrophoresis gels, run at 35 mA and transferred to Immobilon-P polyvinylidene difluoride (Millipore) membrane in a minitrans-blot cell (Amersham) at room temperature in a buffer containing 25 mM Tris-HCl (pH 8.3), 192 mM glycine, and 10% methanol for 1 h and 30 min at 500 mA. To block non-specific binding sites, dried membranes were incubated in blocking solution containing 0.1% polyoxyethylenesorbitan monolaureate (Tween-20), 4% non-fat milk in PBS for 1 h at room temperature. Membranes were subsequently incubated with PBS/0.1% Tween-20 solution supplemented with the following preparation of antibodies: monoclonal 4B12 antibody (0.3 μg/ml) anti-rat Rab27a [34], monoclonal antibody anti-myc-tag (0.3 μg/ml) purchased from Oncogene (Cambridge, MA, USA) or polyclonal anti-calnexin antibody (1:5,000) purchased from StressGene (Victoria, BC, Canada). The mixture was incubated with the primary antibody with gentle agitation for 1 h at room temperature, rinsed and washed with PBS containing 0.1% Tween-20 for 15 min, 3 times. Membranes were then incubated with horseradish peroxidase-coupled secondary antibody (Dako). The blots were washed as described above and bands were visualised by chemiluminescence using SuperSignal West Pico Chemiluminescence Substrate (Pierce) according to the instructions supplied by the manufacturer. All blots were calibrated with prestained molecular weight markers (Bio-Rad Laboratories).

Cell culture, transfections and labelling
COS-7 cells were maintained in Dulbecco's modified Eagle's medium supplemented with 10% fetal bovine serum. Transfections were performed using lipofectamine (Qiagen). Total amounts of transfected DNA were 1 μg/6-cm dish. For pulse-chase experiments, cells were washed with methionine/cysteine-free medium and subsequently incubated with 140 μCi of $[^{35}S]$methionine/cysteine per 6-cm dish for 2 h. After this, cells were washed three times in PBS, and further maintained in normal Dulbecco's modified Eagle's medium supplemented with 10% fetal bovine serum. At indicated time points (0, 30 min, 3, 5, 8 and 22 h), cells were lysed by incubation in buffer containing 50 mM Tris-HCl (pH 7.5), 100 mM NaCl, 1 mM phenyl-methylsulfonyl fluoride, 10 μg/ml leupeptin, 10 μg/ml aprotinin, 10 μg/ml pepstatin, 1 mM DTT and 1% NP-40 for 20 min on ice followed by 5–10 s of sonication. After centrifugation at 14,000 rpm, equal amounts of radioactive lysates were incubated under agitation with 5 μg of 4B12 antibody for 1 h at RT, after lowering the concentration of NP-40 to 0.5% by dilution. Subsequently, 30 μl of protein G-Sepharose beads were added to the radioactive material and incubated overnight at 4°C, while rocking. Then beads were washed four times in PBS, denatured in SDS-containing sample buffer and loaded on a 12%

SDS-polyacrylamide gel, transferred onto 3 MM Whatman paper and quantified using a Storm system (Amersham).

Fundus photography

Fundus photographs of mice were taken using a small animal fundus camera (Kowa Genesis) according to John and co-workers [29]. In order to have a better magnification and focal depth of the fundus, the camera was used in conjunction with an external 90 diopter condensing lens (Volk). This condensing lens was mounted between the camera and the mouse eye. The lens was placed about 5 cm below the camera. All the photographs were taken without anesthesia and with mice's vibrissae trimmed to avoid ocular clouding and obscuring photograph problems. Pupils were dilated with a drop of 1% Mydriacyl (Alcon Laboratories) 20–30 min before taking the photographs. For conventional photography of the fundus, Kodak 200 ASA slide film was used. The photographic flash on the power pack was set up for its highest level (position 6–7) for C57BL/6J mice as the highest intensity of light produced better results on pigmented mice. The mice were held beneath the external lens and the focusing was achieved by moving the mouse. To reduce the light reflection, a major problem of this technique, the position of the eye was very important. Accordingly, the procedure involved focusing through an off central position of the ocular globe.

Fluorescein angiography

The retinal angiography was performed using the general fundus photography procedure. The camera was set up for angiography through addition of an emission barrier filter specific for fluorescein emission and the power pack was set up for fluorescein angiography by changing the excitation light to fluorescein excitation. For this type of photography Kodak black and white Tmax 400 ASA professional film was used. The photographic flash on the power pack was set up for its highest level (position 6–7). Mice were intraperitoneally injected with 20% injectable sodium fluorescein (Faure) at a dose of 10 μl per 5–6 g body weight [44]. Photographs were taken at several intervals, starting at 30 s post-injection.

Electroretinography

ERGs were obtained according to previously reported procedures [45]. Briefly, before anesthesia with ketamine (66.7 mg/kg), xylazine (11.7 mg/kg), and atropine (1 mg/kg), the pupils of dark-adapted mice were dilated. The ERG equipment consisted of a Ganzfeld bowl, a DC amplifier, and a PC-based control and recording unit (Multiliner Vision, Jaeger/Toennies, Hoechberg, Germany). Band-pass filter cut-off frequencies were 0.1 and 3000 Hz. Single flash recordings were obtained both under dark-adapted (scotopic) and light-adapted (photopic) conditions. Light adaptation before the photopic session was performed with a background illumination of 30 cd/m^2 for 10 minutes. Single flash stimulus intensities were increased from 10^{-4} cd*s/m^2 to 25 cd*s/m^2, divided into ten steps of 0.5 and 1 log cd*s/m^2. Ten responses were averaged with an inter-stimulus interval (ISI) of either 5s or 17s (for 1, 3, 10, 25 cd*s/m^2).

Histology

Eyes were fixed in 4% paraformaldehyde, 5% glutaraldehyde and 0.1 M cacodylate buffer for 1 h. Subsequently, the eyes were cut in half and the anterior segment was removed. Fixed eyes were washed three times for 10 min at room temperature with PBS. Specimen were embedded in paraffin, sectioned to 3–5 μm thickness and stained with hematoxylin and eosin according to standard procedures.

List of abbreviations

CHM, choroideremia; REP, Rab Escort Protein; CTL, cytotoxic T-lymphocyte; GS, Griscelli syndrome; PCR, polymerase chain reaction; PBS, phosphate buffered-saline; Hprt, Hypoxanthine phosphoribosyl transferase.

Authors' contributions

JSR designed, performed and analysed all but the ERG experiments, RA generated the transgenic lines and performed some screenings, GBJ and MS performed the ERG experiments, CH and MCS designed, analysed and coordinated the study. All authors read and approved the study.

Acknowledgements

References

1. Zerial M, McBride H: **Rab proteins as membrane organizers.** *Nat Rev Mol Cell Biol* 2001, **2:**107-17
2. Pfeffer SR: **Rab GTPases: specifying and deciphering organelle identity and function.** *Trends Cell Biol* 2001, **11:**487-91
3. Nagata K, Satoh T, Itoh H, Kozasa T, Okano Y, Doi T, Kaziro Y, Nozawa Y: **The ram: a novel low molecular weight GTP-binding protein cDNA from a rat megakaryocyte library.** *FEBS Lett* 1990, **275:**29-32
4. Nagata K, Itoh H, Katada T, Takenaka K, Ui M, Kaziro Y, Nozawa Y: **Purification, identification, and characterization of two GTP-binding proteins with molecular weights of 25,000 and 21,000 in human platelet cytosol. One is the rap1/smg21/Krev-1 protein and the other is a novel GTP-binding protein.** *J Biol Chem* 1989, **264:**17000-5
5. Seabra MC: **Membrane association and targeting of prenylated Ras-like GTPases.** *Cell Signal* 1998, **10:**167-72
6. Pereira-Leal JB, Hume AN, Seabra MC: **Prenylation of Rab GTPases: molecular mechanisms and involvement in genetic disease.** *FEBS Lett* 2001, **498:**197-200
7. Seabra MC: **Nucleotide dependence of Rab geranylgeranylation. Rab escort protein interacts preferentially with GDP-bound Rab.** *J Biol Chem* 1996, **271:**14398-404
8. Seabra MC, Brown MS, Slaughter CA, Sudhof TC, Goldstein JL: **Purification of component A of Rab geranylgeranyl transferase: possible identity with the choroideremia gene product.** *Cell* 1992, **70:**1049-57

9.   Anant JS, Desnoyers L, Machius M, Demeler B, Hansen JC, Westover KD, Deisenhofer J, Seabra MC: **Mechanism of Rab geranylgeranylation: formation of the catalytic ternary complex.** *Biochemistry* 1998, **37:**12559-68

10. Seabra MC, Goldstein JL, Sudhof TC, Brown MS: **Rab geranylgeranyl transferase. A multisubunit enzyme that prenylates GTP-binding proteins terminating in Cys-X-Cys or Cys-Cys.** *J Biol Chem* 1992, **267:**14497-503

11. Thoma NH, Iakovenko A, Goody RS, Alexandrov K: **Phosphoisoprenoids modulate association of Rab geranylgeranyltransferase with REP-1.** *J Biol Chem* 2001, **276:**48637-43

12. Alexandrov K, Horiuchi H, Steele-Mortimer O, Seabra MC, Zerial M: **Rab escort protein-1 is a multifunctional protein that accompanies newly prenylated rab proteins to their target membranes.** *Embo J* 1994, **13:**5262-73

13. Wilson AL, Erdman RA, Maltese WA: **Association of Rab1B with GDP-dissociation inhibitor (GDI) is required for recycling but not initial membrane targeting of the Rab protein.** *J Biol Chem* 1996, **271:**10932-40

14. Cremers FP, Armstrong SA, Seabra MC, Brown MS, Goldstein JL: **REP-2, a Rab escort protein encoded by the choroideremia-like gene.** *J Biol Chem* 1994, **269:**2111-7

15. Seabra MC: **New insights into the pathogenesis of choroideremia: a tale of two REPs.** *Ophthalmic Genet* 1996, **17:**43-6

16. Seabra MC, Ho YK, Anant JS: **Deficient geranylgeranylation of Ram/Rab27 in choroideremia.** *J Biol Chem* 1995, **270:**24420-7

17. Seabra MC, Brown MS, Goldstein JL: **Retinal degeneration in choroideremia: deficiency of rab geranylgeranyl transferase.** *Science* 1993, **259:**377-81

18. Feig LA: **Tools of the trade: use of dominant-inhibitory mutants of Ras-family GTPases.** *Nat Cell Biol* 1999, **1:**E25-7

19. Kluppel M, Beermann F, Ruppert S, Schmid E, Hummler E, Schutz G: **The mouse tyrosinase promoter is sufficient for expression in melanocytes and in the pigmented epithelium of the retina.** *Proc Natl Acad Sci U S A* 1991, **88:**3777-81

20. Beermann F, Schmid E, Schutz G: **Expression of the mouse tyrosinase gene during embryonic development: recapitulation of the temporal regulation in transgenic mice.** *Proc Natl Acad Sci U S A* 1992, **89:**2809-13

21. Hogan B, Bedington R, Costantini F, Lacy E: **Manipulating the Mouse Embryo, A Laboratory Manual:** *Cold Spring Harbor Laboratory Press;* 1994

22. Fregien N, Davidson N: **Activating elements in the promoter region of the chicken beta-actin gene.** *Gene* 1986, **48:**1-11

23. Niwa H, Yamamura K, Miyazaki J: **Efficient selection for high-expression transfectants with a novel eukaryotic vector.** *Gene* 1991, **108:**193-9

24. Hammer RE, Krumlauf R, Camper SA, Brinster RL, Tilghman SM: **Diversity of alpha-fetoprotein gene expression in mice is generated by a combination of separate enhancer elements.** *Science* 1987, **235:**53-8

25. Overbeek PA, Lai SP, Van Quill KR, Westphal H: **Tissue-specific expression in transgenic mice of a fused gene containing RSV terminal sequences.** *Science* 1986, **231:**1574-7

26. Wilson SM, Yip R, Swing DA, O'Sullivan TN, Zhang Y, Novak EK, Swank RT, Russell LB, Copeland NG, Jenkins NA: **A mutation in Rab27a causes the vesicle transport defects observed in ashen mice.** *Proc Natl Acad Sci U S A* 2000, **97:**7933-8

27. Menasche G, Pastural E, Feldmann J, Certain S, Ersoy F, Dupuis S, Wulffraat N, Bianchi D, Fischer A, Le Deist F, *et al:* **Mutations in RAB27A cause Griscelli syndrome associated with haemophagocytic syndrome.** *Nat Genet* 2000, **25:**173-6

28. Barral DC, Ramalho JS, Anders R, Hume AN, Knapton HJ, Tolmachova T, Collinson LM, Goulding D, Authi KS, Seabra MC: **Functional redundancy of Rab27 proteins and the pathogenesis of Griscelli syndrome.** *J Clin Invest* 2002, **110:**247-251

29. Hawes NL, Smith RS, Chang B, Davisson M, Heckenlively JR, John SW: **Mouse fundus photography and angiography: a catalogue of normal and mutant phenotypes.** *Mol Vis* 1999, **5:**22

30. van der Sluijs P, Hull M, Webster P, Male P, Goud B, Mellman I: **The small GTP-binding protein rab4 controls an early sorting event on the endocytic pathway.** *Cell* 1992, **70:**729-40

31. Bucci C, Parton RG, Mather IH, Stunnenberg H, Simons K, Hoflack B, Zerial M: **The small GTPase rab5 functions as a regulatory factor in the early endocytic pathway.** *Cell* 1992, **70:**715-28

32. Ullrich O, Reinsch S, Urbe S, Zerial M, Parton RG: **Rab11 regulates recycling through the pericentriolar recycling endosome.** *J Cell Biol* 1996, **135:**913-24

33. Andre P, Boretto J, Hueber AO, Regnier-Vigouroux A, Gorvel JP, Ferrier P, Chavrier P: **A dominant-negative mutant of the Rab5 GTPase enhances T cell signaling by interfering with TCR down-modulation in transgenic mice.** *J Immunol* 1997, **159:**5253-63

34. Hume AN, Collinson LM, Rapak A, Gomes AQ, Hopkins CR, Seabra MC: **Rab27a regulates the peripheral distribution of melanosomes in melanocytes.** *J Cell Biol* 2001, **152:**795-808

35. Griscelli C, Durandy A, Guy-Grand D, Daguillard F, Herzog C, Prunieras M: **A syndrome associating partial albinism and immunodeficiency.** *Am J Med* 1978, **65:**691-702

36. Klein C, Philippe N, Le Deist F, Fraitag S, Prost C, Durandy A, Fischer A, Griscelli C: **Partial albinism with immunodeficiency (Griscelli syndrome).** *J Pediatr* 1994, **125:**886-95

37. Bahadoran P, Aberdam E, Mantoux F, Busca R, Bille K, Yalman N, de Saint-Basile G, Casaroli-Marano R, Ortonne JP, Ballotti R: **Rab27a: A key to melanosome transport in human melanocytes.** *J Cell Biol* 2001, **152:**843-50

38. Wu X, Rao K, Bowers MB, Copeland NG, Jenkins NA, Hammer JA 3rd: **Rab27a enables myosin Va-dependent melanosome capture by recruiting the myosin to the organelle.** *J Cell Sci* 2001, **114:**1091-100

39. Stinchcombe JC, Barral DC, Mules EH, Booth S, Hume AN, Machesky LM, Seabra MC, Griffiths GM: **Rab27a is required for regulated secretion in cytotoxic T lymphocytes.** *J Cell Biol* 2001, **152:**825-34

40. Haddad EK, Wu X, Hammer JA 3rd, Henkart PA: **Defective granule exocytosis in Rab27a-deficient lymphocytes from Ashen mice.** *J Cell Biol* 2001, **152:**835-42

41. Hofmann SL, Russell DW, Brown MS, Goldstein JL, Hammer RE: **Overexpression of low density lipoprotein (LDL) receptor eliminates LDL from plasma in transgenic mice.** *Science* 1988, **239:**1277-81

42. Palmiter RD, Norstedt G, Gelinas RE, Hammer RE, Brinster RL: **Metallothionein-human GH fusion genes stimulate growth of mice.** *Science* 1983, **222:**809-14

43. Strom M, Hume AN, Tarafder AK, Barkagianni E, Seabra MC: **A family of Rab27-binding proteins: Melanophilin links Rab27a and myosin Va function in melanosome transport.** *J Biol Chem* 2002, **277:**25423-30

44. Okamoto N, Tobe T, Hackett SF, Ozaki H, Vinores MA, LaRochelle W, Zack DJ, Campochiaro PA: **Transgenic mice with increased expression of vascular endothelial growth factor in the retina: a new model of intraretinal and subretinal neovascularization.** *Am J Pathol* 1997, **151:**281-91

45. Seeliger MW, Grimm C, Stahlberg F, Friedburg C, Jaissle G, Zrenner E, Guo H, Reme CE, Humphries P, Hofmann F, *et al:* **New views on RPE65 deficiency: the rod system is the source of vision in a mouse model of Leber congenital amaurosis.** *Nat Genet* 2001, **29:**70-4